

Speckle reduction for multi-polarimetric SAR image with the similarity of the scattering

YANG Xuezhi¹, ZUO Meixia¹, LANG Wenhui¹, ZHANG Xi², MENG Junmin²

1. School of Computer and Information, Hefei University of Technology, Hefei 230009, China;

2. The First Institute of Oceanography, SOA, Qingdao 266061, China

Abstract: The speckle in polarimetric Synthetic Aperture Radar (SAR) image has seriously affected the effectiveness in extracting information. For this reason, a novel method based on the similarity of the scattering for speckle reduction is proposed. This method combines the similarity of the scattering properties and the redundant information in SAR image, and applies the Wishart distribution of SAR data to implement the measurement of the similarity. It then averages the covariance matrices with the weights according to the similarity between the matrices, leading to efficient reduction of the speckle in SAR image. The method processes each element of the covariance matrices, given its advantage in preserving polarimetric properties. Compared with the existing methods, including the Polarimetric Whitening Filter (PWF) and the polarimetric Lee filter, the implementation result indicates that the proposed algorithm is effective in improving the performance of despeckling and details preservation.

Key words: SAR, multi-polarimetric, speckle reduction, scattering character, similarity

CLC number: TP751 **Document code:** A

Citation format: Yang X Z, Zuo M X, Lang W H, Zhang X and Meng J M. 2012. Speckle reduction for multi-polarimetric SAR image with the similarity of the scattering. *Journal of Remote Sensing*, 16(1): 105–115

1 INTRODUCTION

Synthetic aperture radar (SAR) is a coherent wave imaging system with high azimuth resolution and distance resolution (Zhu, et al., 2009). Multi-polarimetric SAR image provides multidimensional information of the target. Recently, it has been widely used in eco-hydrology, sea ice research, ocean monitoring and many other research domains. Speckle is an inherent noise formed in SAR imaging process, which seriously affects the following manual and automatic interpretation of SAR image (Maitre & Sun, 2005). Therefore, speckle reduction of polarimetric SAR image has become a key issue in SAR image processing.

In the early research of multi-polarimetric speckle reduction, many methodologies were presented and the average filter was often used, which takes the average value in the neighborhood window of pixels to estimate the current point. Although the method reduces the speckle to some extent, it does not maintain the spatial resolution and retain the details in the image effectively (Bouchemakh, et al., 2008). The polarimetric whitening filter (PWF) was proposed by Novak and Burl (1990). It combines and weights the polarimetric covariance matrices of all polarimetric channels, and then uses the full polarimetric data to generate an intensity image (Touzi & Lopes, 1994; Pi, et al., 2002; Liu, et al., 2003).

However, this method reduces the correlations among all channels and loses the polarimetric information. In recent years, Lee, et al.(1991) used the multiplicative noise model and proposed the Lee filter in polarimetric field, which weights the covariance matrix optimally under a premise of minimum mean square error (Jiang, et al., 2009). Compared with the earlier methodologies, Lee filter has greatly improved the capacity of speckle reduction, but it still does not maintain image details well. In sum, most of the available methods can not filter every element of the covariance matrices singly, so they can not preserve polarimetric information effectively, indicates that they are detrimental to post-processing, such as segmentation, classification and other interpretation about polarimetric SAR images.

According to the analysis, the common problem of the speckle reduction methods lies in their inefficiencies in details retaining and the polarimetric information preserving, which are uncondusive to the interpretation of SAR image. For this reason, a new speckle reduction methodology with polarization information preserving ability is proposed. From the perspective of similarity of the scattering properties, this method combines the Wishart distribution of SAR data and proposes the measurement of the similarity as well as introduces the similarity into the process of speckle reduction. Then, it proposes a speckle reduction mechanism in polarization domain.

Received: 2010-11-26; **Accepted:** 2011-02-23

Foundation: National Natural Science Foundation of China (No. 41076120, 60890075); Science and Technological Fund of Anhui Province for Outstanding Youth (No. 10040606Y09); Training Program for Distinguished Young Scholars, School of Computer and Information, Hefei University of Technology (No. 2010HGXJ0017); Talents Development Grants of Anhui Province (No. 2008Z054); SRF for ROCS, SEM

First author biography: YANG Xuezhi (1970—), male, Ph.D., professor, his research interests are image processing, pattern recognition and synthetic aperture radar image interpretation. Related papers have been published more than 10, with some articles included by the SCI. E-mail: hfut.cv@gmail.com

2 SPECKLE REDUCTION OF THE POLARIMETRIC SAR IMAGE

2.1 The statistical analysis of the polarimetric SAR image

When the SAR observes the targets in a particular position and frequency (Oliver & Quegan, 1998), the full polarimetric information of the objects can be expressed by Sinclair scattering matrix in the linear polarization base as follows.

$$S = \begin{bmatrix} S_{hh} & S_{hv} \\ S_{vh} & S_{vv} \end{bmatrix} \quad (1)$$

where S_{vh} is the scattering element which means transmit horizontal polarimetric waves and received in vertical channel, the other three elements are similarly defined. In the case of the reciprocal backscattering, $S_{hv}=S_{vh}$. The observed value in SAR image can be expressed by the three-dimensional target vector k

$$k = [S_{hh} \ \sqrt{2}S_{hv} \ S_{vv}]^T \quad (2)$$

The covariance matrix can represent the polarimetric information of the target, which is defined as

$$C = k \cdot k^H = \begin{bmatrix} |S_{hh}|^2 & \sqrt{2}S_{hh}S_{hv}^* & S_{hh}S_{vv}^* \\ \sqrt{2}S_{hv}S_{hh}^* & 2|S_{hv}|^2 & \sqrt{2}S_{hv}S_{vv}^* \\ S_{vv}S_{hh}^* & \sqrt{2}S_{vv}S_{hv}^* & |S_{vv}|^2 \end{bmatrix} \quad (3)$$

where the superscript "T" denotes the transpose of the matrix, and the superscript "H" denotes the complex conjugate and transpose. Weight the polarimetric SAR scattering vector can obtain the total power image, also known as the span, which reflects the scattering information of the target. Namely, it contains the diagonal elements of the covariance matrix and calculated as

$$p_{span} = |S_{hh}|^2 + 2|S_{hv}|^2 + |S_{vv}|^2 \quad (4)$$

The results show that the covariance matrix can be modeled by complex Wishart distribution with n degrees of freedom, $W_C(n, \Sigma)$ (Lee, et al., 1999). The probability density function is given by

$$p(C) = \frac{n^n |C|^{n-q} \exp(-tr(n(\Sigma)^{-1} \cdot C))}{K(n, q) \cdot |\Sigma|^n} \quad (5)$$

where $K(n, q) = \pi^{\frac{q(q-1)}{2}} \prod_{i=1}^q \Gamma(n-i+1)$ is the normalization factor, $\Sigma = E(k \cdot k^H)$ is the spatial statistical average of the covariance matrix, tr is the trace of matrix, q is the number of polarization channels, in the condition of the polarization and reciprocity, $q=3$. $\Gamma()$ is the Gamma function.

2.2 The similarity of the scattering properties in polarimetric SAR image

Multi-polarization SAR image blocks have redundancy information, as shown in Fig. 1, in which the blocks with the same color indicate that these regions are similar (Buades, et al., 2005a, 2005b; Yang & Clausi, 2009). Scattering properties corresponding to the similar SAR image blocks should have a certain similarity.

If a set of covariance matrices is $\{C_1, C_2, \dots, C_m\}$, with m is the number of the pixels corresponding to the regions of SAR image, according Eq. (5), the conditional probability density of the

covariance matrix is (Lee, et al., 1999)

$$p(C_x | C_y) = \frac{n^n |C_x|^{n-q} \exp(-tr(nC_y^{-1} \cdot C_x))}{K(n, q) \cdot |C_y|^n} \quad (6)$$

From a computational point of view, it is generally preferable to deal with log-likelihood function, let $L(C_x | C_y)$ instead of the expression given in Eq. (7).

$$L(C_x | C_y) = -n \ln |C_y| - ntr(C_y^{-1} \cdot C_x) + (n-q) \ln |C_x| - \ln K(n, q) \quad (7)$$

Let C_y be the center of the y^{th} cluster and $y \neq x$. When the prior probability is unknown, taking the opposite of the expression of relation Eq. (7) and removing terms that independent on the cluster under test, the distance between the covariance matrix C_x and C_y is then defined as

$$d(C_x, C_y) = \ln |C_y| + tr(C_y^{-1} \cdot C_x) \quad (8)$$

According to Bayesian optimal decision theory, for the current covariance matrix C_x , if the $d(C_x, C_y)$ is the minimum distance cluster in all the $y \in \{1, 2, \dots, m\}$ and $y \neq x$, then C_x is assigned to the y^{th} cluster. Now it shows high similarity between the covariance matrix C_x and C_y . Therefore, the distance d can be seen as the similarity measurement parameter about the scattering characteristics. If d is smaller, their scattering properties are more similar.

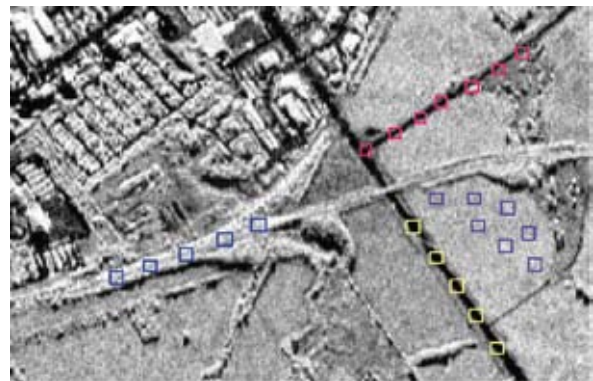


Fig. 1 The redundant information in SAR image

2.3 The speckle reduction based the similarity of the scattering characteristics

This work introduces the similarity and restores the scattering properties by weighting additionally averaging the global polarimetric data. The weight value depends on the similarity of the scattering properties and larger similarity leads to higher weigh, indicating data with higher similarity would have greater contribution in the process of the speckle reduction. The process is expressed as

$$NL(C_x) = \frac{1}{Z(x)} \sum_{C_y \in Y} w(C_x, C_y) C_y \quad (9)$$

where C_x is the covariance matrix to be processed, C_y are all the covariance matrices in the current filter window excluding C_x , $w(C_x, C_y)$ is the weight selected when weighting and averaging. As observed in Eq. (10), it depends on the similarity between the C_x and C_y .

The weight can be written as

$$w(C_x, C_y) = \exp\left(-\frac{(\ln|C_y| + \text{tr}(C_y^{-1}C_x))^2}{h^2}\right) \quad (10)$$

where the normalization factor $Z(x)$ in Eq. (9) is

$$Z(x) = \sum_{C_y \in Y} \exp\left(-\frac{(\ln|C_y| + \text{tr}(C_y^{-1}C_x))^2}{h^2}\right) \quad (11)$$

where h is an experience parameter which controls the degree of the filtering.

2.4 The process and steps of the algorithm

The process and the details of the algorithm are as follows. When calculating the distance between the pending matrix and other matrices, the matrix to be processed will be assigned as the center firstly and then selects a small window as the neighborhood window. Then slide the neighborhood window with the limit of the filtering window. Each matrix in the filtering window will be the center data of the search window, and the distance between the center data and the matrix to be processed will be replaced by the average distance, which is between the polarimetric data in the corresponding position of its own search window and the neighborhood window.

The specific steps are shown as below:

Step 1 Extract the original multi-polarization SAR image data, and obtain polarization scattering characteristics of targets;

Step 2 Because larger size window will enhance the filtering, while smaller window will maintain the details, in the experiment, the filtering window is set to 5×5 ; the neighborhood window is selected by 3×3 , which is the size of the search window; the smoothing parameter h is 0.5;

Step 3 Slide the search window in the filtering window, and calculate the distance between each center matrices in the search window and the covariance matrix to be processed by using Eq. (8). This distance is replaced by the average distance between the matrices in the corresponding position of its own search window and the neighborhood window;

Step 4 Take the distance obtained in **Step 3** into Eq. (10) to obtain the weights of each matrix in the filtering window to the matrix to be processed, which is the measurement of the similarity;

Step 5 Weight and average the covariance matrix in the search window according to Eq. (9) to obtain the restored matrix;

Step 6 In accordance with the above steps, all of the elements of the covariance matrix should be processed in a similar manner. Then the total power is calculated according to Eq. (4). Finally, the false color synthetic images before and after speckle filtering can be obtained by polarizations synthesized.

3 TESTING AND EVALUATION

3.1 The effect assessment and analysis about the speckle reduction

In order to evaluate the effect of speckle reduction objectively, several indicators are used in this paper.

(1) The Equivalent Number of Looks (ENL) is a measurement of the relative strength index about the speckle intensity in SAR image (Wang, et al., 2004). In a homogeneous region it defined as

$$\text{ENL} = \frac{\mu^2}{\sigma^2} \quad (12)$$

where μ and σ are the respective local mean and standard deviation in SAR image. A large ENL indicates good speckle reduction performance. Speckle reduction factor β is defined as

$$\beta = \frac{1}{\sqrt{\text{ENL}}} \quad (13)$$

(2) The degree of the mean deviation is an indicator of the details preservation(Wang, et al, 2009). It is defined as

$$\text{Devi} = \frac{\mu'_i - \mu_i}{\mu_i} \quad (14)$$

where μ_i and μ'_i are the image mean value before and after filtering respectively. If a image has not been any processed, $\text{Devi}=0$. After filtering, if the value is close to zero, it indicates the details kept well.

(3) The polarization characteristics signatures can evaluate the preservation of polarimetric information before and after filtering. The signatures response the received power in any combination cases about the SAR antennas, i.e.

$$P(\delta_r, \varphi_r, \delta_t, \varphi_t) = k'(\lambda, \theta, \varphi) \mathbf{J}_r^T \mathbf{K}' \mathbf{J}_t \quad (15)$$

where (δ_r, φ_r) and (δ_t, φ_t) are the polarization ellipse parameters of the receiving electromagnetic wave and the transmitting. δ_r and φ_r are the ellipticity angle and azimuth of the transmitting antenna, respectively. $k'(\lambda, \theta, \varphi)$ is a constant related by the effective area of the antenna and waveguide. \mathbf{J}_r and \mathbf{J}_t describe the Stokes polarization vector in the case of (δ_r, φ_r) and (δ_t, φ_t) respectively, independent of the target scattering. \mathbf{K}' is the Kennaugh matrix of the target. The superscript "T" says the vector transpose. If in the case of caring the relative value of the received power, the constants can be omitted to simplify the calculation. The polarization state of the transmitting antenna and the receiving can be any value within the effective range. When $\delta_r = \delta_t$ and $\varphi_r = \varphi_t$, the same polarization state of the two is called the co-polarization, When $\delta_r = -\delta_t$ and $\varphi_r = \pi - \varphi_t$, this orthogonal polarization state of the two is called cross-polarization. It can obtain the three-dimensional polarization characteristics signatures by the received power of the electromagnetic wave. From the above, the signatures are determined by the Kennaugh matrix of the target and the Kennaugh matrix also contains the polarization information, so the polarization characteristics signatures can represent the polarization information of the objects.

3.2 The experiments of the despeckling about the multi-polarimetric SAR image

The following test data used in experiments are carried out from San Francisco Bay polarimetric SAR data, which is acquired by the EMISAR in L-band and from the U.S. Jet Propulsion Laboratory. The image regions composed by the Pacific in the upper left, the Golden Gate Bridge in the upper right and the San Francisco's urban in the lower right. The size of the data area is selected by 512×512 . Fig. 2 shows the polarization false color synthetic images processed by several methods above.

From the visual point, these methods have some degree of speckle reduction. It can be seen that the PWF has a bad performance, as much speckle still exists in the sea-level area. This is because the PWF obtains the speckle reduction image by combination the data from all channels. The polarimetric Lee filter reduces the speckle well, but more details in the urban areas are lost, as shown in Fig. 2(c) that the details in the red circle have been blurred. Be-

cause the performance of the polarimetric Lee filter depends on the size of the filter window. If the window is too small, the image will be under-filtered; if the window is too big, over-filtering may result in blurring. In addition, the above two methods introduce crosstalk between channels (Zhou, et al., 2008), leading to the loss of polarization information.

The proposed method has improved the performance of filtering compared with the PWF and the polarimetric Lee filter. Firstly, the image structure in the upper left is relatively simple. The speckle is less, and the image is smoother, as shown in the white box in Fig. 2 (d). Secondly, the area in the lower of the image has com-

plex structures and more details, and its line structure is clearer, as shown in the red circle in Fig. 2 (d). In order to compare the ability about maintaining the details, Fig. 2 (e)-(h) shows the enlarged images corresponding areas in the right box in Fig. 2 (a) after filtering by various methods. It can be seen that the details in Fig. 2 (h) are more prominent and the image quality is the best.

From the global and local perspective, the proposed method is significantly better than the existing methods, including the PWF and the polarization Lee filter. The new method processes each element of the covariance matrix separately, so it better retains the polarization information. Fig. 3 shows the polarization characteristics

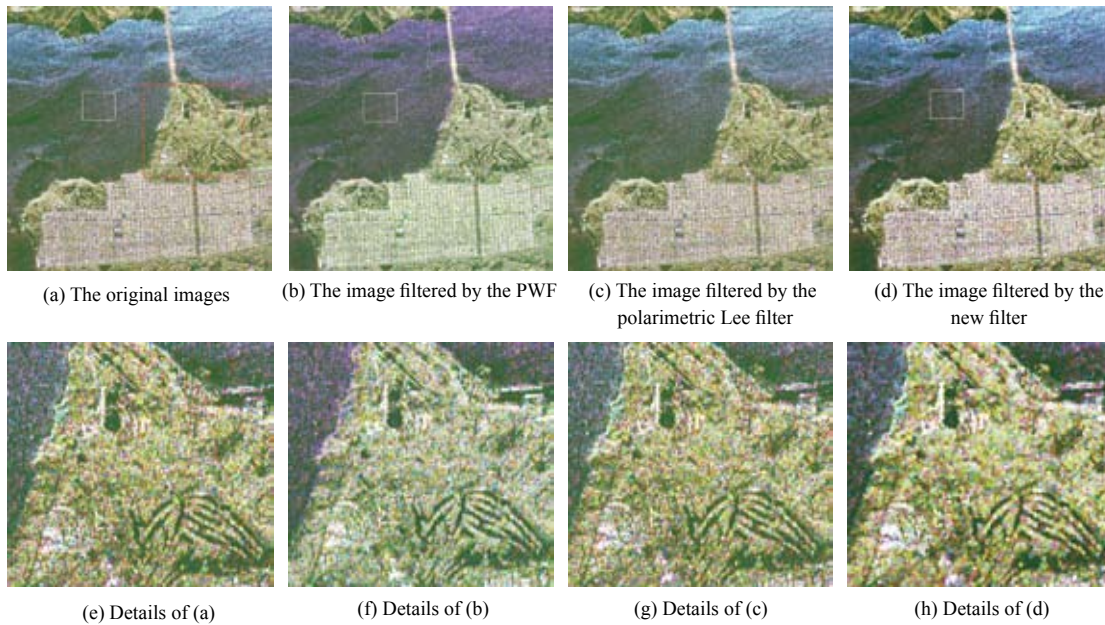


Fig. 2 The results of the false color synthetic SAR images

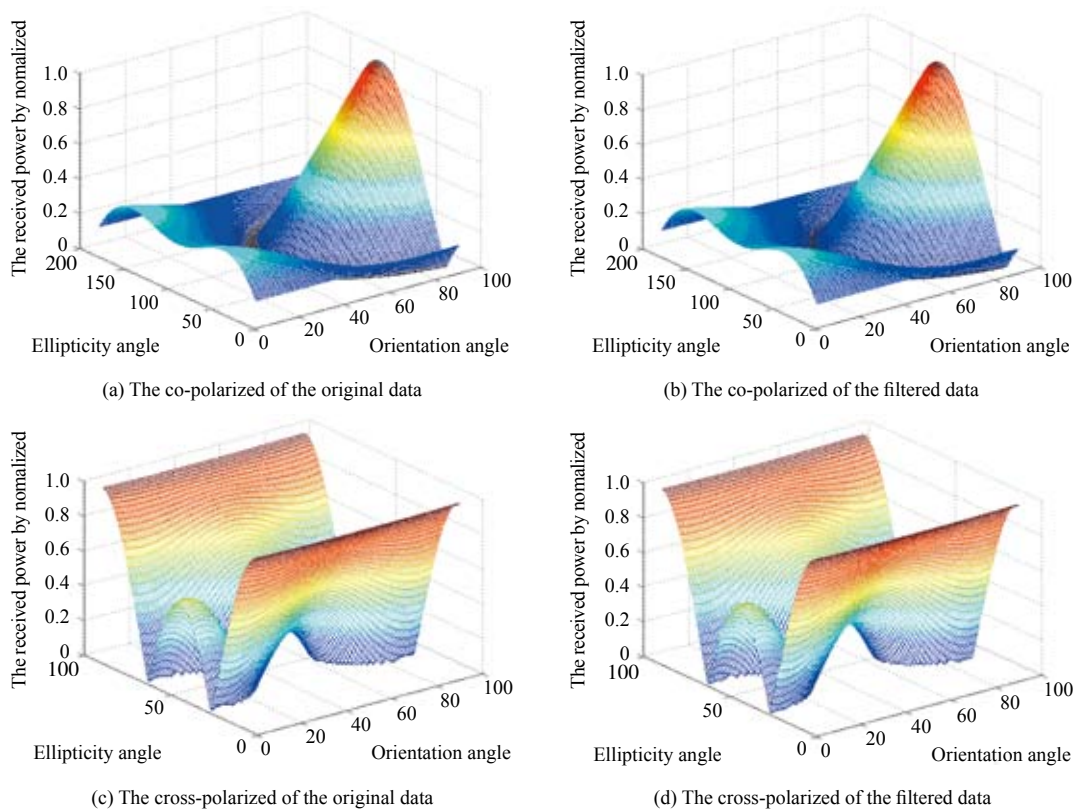


Fig. 3 The polarization characteristics signatures

signatures in the white box areas corresponding to the original and the filtered data. Both the co-polar and the cross-polar signatures of the original data and the filtered data have high consistency, which demonstrates that the new method can maintain polarization information in totality.

In order to quantitatively assess the filters, the above indicators ENL and Devi are used. First, in order to evaluate the performance of the despeckling quantitatively, the mean value (μ), the standard deviation (σ) and the ENL in the areas of left box corresponding to the original image, the images after the process of the PWF and the polarimetric Lee filter respectively shows in Table 1. Then to maintain the level of image detail assessment, the Table 2 shows the Devi value of the original and the filtered images.

As can be seen from the table, in the new method, both σ and β are smaller, ENL is larger compared with the other filters. Therefore, the new filter has good ability of speckle reduction. The Devi value is closest to 0, which shows that the new method has the best ability to preserve the details.

Table 1 Comparison of the speckle reduction of different methods

The polarization false color synthetic images				
	The original	The PWF	The polarimetric Lee filter	The new filter
σ	55.7696	54.1479	54.9324	40.9214
μ	127.3470	92.6229	128.2230	120.3650
ENL	5.2142	2.9260	5.4485	8.6518
β	0.4379	0.5846	0.4284	0.3400

Table 2 Comparison of the ability of retaining the details of different methods

The polarization false color synthetic images				
	The original	The PWF	The polarimetric Lee filter	The new filter
Devi	-0.0251	-0.0276	-0.0207	-0.0200

4 CONCLUSION

In this paper, a new speckle filter for polarimetric SAR data has been presented. It derives parameters for measuring similarity of the scattering characteristics by analyzing the similarity of the scattering about SAR images data, introducing the idea of weighting and averaging in polarization domain and combining the Wishart distribution of the covariance matrix. The effectiveness of this algorithm is demonstrated by using the true polarimetric SAR data. This algorithm performs well both on speckle reduction and on preservation details. In particular, it emphasizes that it can process each element of the covariance matrices, given its potential advantages in preserving polarimetric properties, which facilitates the following processing. However, it should be noted that it will affect the measuring of scattering properties in the search windows when the speckle is serious in SAR images. How to reduce the speckle

effects on the similarity measurement is the further research work.

REFERENCES

- Buades A, Coll B and Morel J M. 2005a. Image denoising by non-local averaging. 2005 IEEE International Conference on Acoustics Speech and Signal Processing. New York: IEEE, 2: 25–28 DOI: 10.1109/ICASSP.2005.1415332
- Buades A, Coll B and Morel J M. 2005b. A review of image denoising algorithms, with a new One. Multiscale Modeling and Simulation, 4(2): 490–530 DOI: 10.1137/040616024
- Bouchemakh L, Smara Y and Boutarfa S. 2008. A comparative study of speckle filtering in polarimetric radar SAR images. Proceedings of the International Conference on Information and Communication Technologies from Theory to Applications ICTTA' 08. New York: IEEE: Piscataway, NJ, USA: 1–6 DOI: 10.1109/ICTTA.2008.4530040
- Jiang Y, Zhang X L and Shi J. 2009. Speckle reduction for polarimetric SAR images by improved lee filter. Journal of University of Electronic Science and Technology of China, 38(1): 5–8
- Lee J S, Grunes M R and De Grandi G. 1999. Polarimetric SAR speckle filtering and its implication for classification. IEEE Trans Geoscience and Remote Sensing, 37(5): 2363–2373 DOI: 10.1109/36.789635
- Liu X Q, Yang Z and Yang R L. 2003. Improvement research of parameter estimation in polarimetric whitening filter of full-polarization SAR image. Acta Electronica Sinica, 31(12): 1795–1799
- Maitre H, Sun H. 2005. Processing of Synthetic Aperture Radar. Beijing: Publishing House of Electronics Industry: 28–30
- Maitre, Sun H and Guan B. 2004. Evaluation for coherent speckle suppression filters of SAR images. Journal of systems Engineering and Electronics, 26(9):1165–1171
- Oliver C and Quegan S. 1998. Understanding Synthetic Aperture Radar Images. Boston: Artechhouse: 209–212
- Pi Y M, Zou Q and Huang S J. 2002. Speckle reduction of polarimetric SAR-polarimetric whitening filter. Journal of Electronics and Information Technology, 24(5): 597–603
- Touzi R and Lopes A. 1994. The principle of speckle filtering in polarimetric SAR imagery. IEEE Transactions on Geoscience and Remote Sensing, 32(5): 1110–1114 DOI: 10.1109/36.312901
- Wang X J, Sun H and Guan B. 2004. Evaluation for coherent speckle suppression filters of SAR images. Systems Engineering and Electronics, 26(9): 1165–1171
- Wang Y, Lu J G and Zhang F. 2009. A new method for evaluating different polarimetric filters. Radio Engineering of China, 39(4): 37–40
- Yang X Z and Clausi D A. 2009. Structure-preserving speckle reduction of SAR images using nonlocal means filters. Image Processing (ICIP), 2009 16th IEEE International Conference on. New York: IEEE, 345 E 47Th St, New York, NY 10017 USA: 2985–2988
- Zhou X G, Kuang G Y and Wan J W. 2008. A review of polarimetric SAR speckle reduction. Journal of Image and Graphics, 13(3): 377–385
- Zhu L, Guo W and Yu W D. 2009. Analysis of SAR satellite development history and tendency. Modern Radar, 31(4): 5–10

采用散射特征相似性的极化SAR图像相干斑抑制

杨学志¹, 左美霞¹, 郎文辉¹, 张晰², 孟俊敏²

1. 合肥工业大学 计算机与信息学院, 安徽 合肥 230009;
2. 国家海洋局第一海洋研究所, 山东 青岛 266061

摘要: 极化合成孔径雷达(SAR)图像的相干斑严重影响图像信息的有效提取, 为此提出一种基于极化散射特性的相干斑抑制方法。该方法结合SAR图像的冗余信息及其散射特性的相似性, 利用Wishart分布对SAR数据的相似性进行度量, 然后依据相似性计算权重对协方差矩阵进行加权平均, 实现对极化SAR图像的相干斑抑制。本文方法对协方差矩阵的各元素单独处理, 因此在极化信息的保留方面尤其优势。通过真实SAR数据的实验表明, 该方法与现有极化白化滤波(PWF)和极化Lee滤波相比, 具有更好的相干斑抑制能力和细节的保持能力。

关键词: 合成孔径雷达, 多极化, 相干斑抑制, 散射特性, 相似性

中图分类号: TP751 **文献标志码:** A

引用格式: 杨学志, 左美霞, 郎文辉, 张晰, 孟俊敏. 2012. 采用散射特征相似性的极化SAR图像相干斑抑制. 遥感学报, 16(1): 105-115
 Yang X Z, Zuo M X, Lang W H, Zhang X and Meng J M. 2012. Speckle reduction for multi-polarimetric SAR image with the similarity of the scattering. Journal of Remote Sensing, 16(1): 105-115

1 引言

合成孔径雷达(SAR)是一种具有很高方位向分辨率及距离向分辨率的相干波成像系统(朱良等, 2009)。多极化SAR图像能提供目标的多维信息, 近年来已被广泛用于生态水文、海洋监测及冰川研究等诸多领域。相干斑是SAR在相干成像过程中所形成的一种固有的类似噪声的现象, 其严重影响SAR图像后续人工判读和计算机自动解译等处理。因此多极化SAR图像相干斑抑制已成为SAR图像处理领域中广为关注的问题(Maitre和孙洪, 2005)。

早期多极化SAR图像相干斑抑制通常采用多视平均的方法, 即利用邻域窗口内数据的均值来估计当前数据点的值。虽然该方法对多极化SAR图像相干斑有一定的抑制作用, 但是在图像空间分辨率及细节信息保持等方面效果不好(Bouchemakh等, 2008), 一定程度上降低了图像质量。Novak和Burl等人提出的极化白

化滤波(PWF)方法(Touzi和Lopes, 1994; 皮亦鸣等, 2002; 刘秀清等, 2003)通过加权组合各极化通道的协方差矩阵元素, 将全极化数据生成一幅强度图像。该方法在抑制图像相干斑的同时也改变了各极化通道之间的相关性, 损失了极化信息。近年来Lee等人利用乘性噪声模型, 提出了极化域中的Lee滤波(江勇等, 2009), 其在最小均方误差的前提下对协方差矩阵进行最优加权。该方法与早期方法相比, 相干斑抑制效果有了较大提高, 但图像细节保持仍不够理想。综合现有方法看来, 大部分算法没有对协方差矩阵的每个元素进行独立处理, 损失了全极化图像的部分极化信息, 不利于极化SAR图像的分割或分类等后期处理。

由此可见, 多极化相干斑抑制现有方法存在的共性问题是不能很好地保持图像细节和极化信息, 因而影响SAR图像的有效解译。对此, 提出一种能够保留极化信息的相干斑抑制新方法。该方法从目标散射特性的相似性角度出发, 有效结合SAR数据的Wishart

收稿日期: 2010-11-26; 修订日期: 2011-02-23

基金项目: 国家自然科学基金(编号: 41076120, 60890075); 安徽省优秀青年科技基金(编号: 10040606Y09); 合肥工业大学计算机与信息学院人才培养计划(编号: 2010HGJ0017); 安徽省人才开发基金(编号: 2008Z054); 教育部留学回国人员科研启动基金

第一作者简介: 杨学志(1970—), 男, 教授。主要研究方向为数字图像处理, 模式识别, 计算机视觉, 合成孔径雷达遥感图像处理, 极区海冰监测及导航技术。已发表相关论文十余篇, 其中多篇被SCI收录。E-mail: hfut.cv@gmail.com。

统计分布，提出散射特性相似性的度量方法，将其相似性引入到相干斑抑制过程进而推导出极化域SAR图像的相干斑抑制机制。实验结果表明，本文方法比常见的传统方法有更好的相干斑抑制效果和图像细节保持能力，同时能够保留SAR图像数据的极化信息。

2 极化SAR图像相干斑抑制

2.1 极化SAR图像统计特性分析

SAR在特定的姿态及观测频率下，目标的全部极化信息由Sinclair散射矩阵表示(Oliver和Quegan, 1998)，对应的S矩阵表达式为

$$\mathbf{S} = \begin{bmatrix} \mathbf{S}_{hh} & \mathbf{S}_{hv} \\ \mathbf{S}_{vh} & \mathbf{S}_{vv} \end{bmatrix} \quad (1)$$

式中， \mathbf{S}_{vh} 表示发射水平极化波时垂直通道接收到的极化分量。对于互易介质，散射矩阵具有对称形式，即 $\mathbf{S}_{hv} = \mathbf{S}_{vh}$ 。SAR图像观测值可由3维目标向量 \mathbf{k} 表示。

$$\mathbf{k} = [\mathbf{S}_{hh} \quad \sqrt{2}\mathbf{S}_{hv} \quad \mathbf{S}_{vv}]^T \quad (2)$$

目标的极化信息可以由协方差矩阵 \mathbf{C} 表示，

$$\mathbf{C} = \mathbf{k} \cdot \mathbf{k}^H = \begin{bmatrix} |\mathbf{S}_{hh}|^2 & \sqrt{2}\mathbf{S}_{hh}\mathbf{S}_{hv}^* & \mathbf{S}_{hh}\mathbf{S}_{vv}^* \\ \sqrt{2}\mathbf{S}_{hv}\mathbf{S}_{hh}^* & 2|\mathbf{S}_{hv}|^2 & \sqrt{2}\mathbf{S}_{hv}\mathbf{S}_{vv}^* \\ \mathbf{S}_{vv}\mathbf{S}_{hh}^* & \sqrt{2}\mathbf{S}_{vv}\mathbf{S}_{hv}^* & |\mathbf{S}_{vv}|^2 \end{bmatrix} \quad (3)$$

式中，上标“T”表示向量的转置；“H”表示矩阵的共轭转置。全极化SAR散射矢量加权得到总功率图像(也称span图)，其反映了目标的散射特性，即协方差矩阵对角线元素之和。计算式为：

$$p_{\text{span}} = |\mathbf{S}_{hh}|^2 + 2|\mathbf{S}_{hv}|^2 + |\mathbf{S}_{vv}|^2 \quad (4)$$

研究表明 n 视的协方差 \mathbf{C} 服从Wishart分布(Lee等, 1999)，即 $W_C(n, \Sigma)$ ，其概率密度函数：

$$p(\mathbf{C}) = \frac{n^q |\mathbf{C}|^{n-q} \exp(-tr(n(\Sigma)^{-1} \cdot \mathbf{C}))}{K(n, q) \cdot |\Sigma|^n} \quad (5)$$

式中， $K(n, q) = \pi^{\frac{q(q-1)}{2}} \prod_{i=1}^q \Gamma(n-i+1)$ ，表示归一化因子； $\Sigma = E(\mathbf{k} \cdot \mathbf{k}^H)$ 为多视协方差矩阵的空间统计平均； tr 表示矩阵的迹； q 为极化通道数，对于极化互易情况 $q=3$ ； $\Gamma()$ 表示Gamma函数。

2.2 极化SAR图像散射特性的相似性

多极化SAR图像块间的信息具有冗余性，如图

1所示。相同颜色方块表明这些区域块具有相似性(Buades等, 2005a, 2005b; Yang和Clausi, 2009)。并且认为相似的SAR图像块对应的散射特性具有一定的相似性。

记图像某区域对应的散射协方差矩阵集为 $\{\mathbf{C}_1, \mathbf{C}_2, \dots, \mathbf{C}_m\}$ ， m 为像素点个数。对于 $1 \leq x, y \leq m$ ，由式(5)可得协方差矩阵的条件概率密度(Lee等, 1999)

$$p(\mathbf{C}_x | \mathbf{C}_y) = \frac{n^q |\mathbf{C}_x|^{n-q} \exp(-tr(n\mathbf{C}_y^{-1} \cdot \mathbf{C}_x))}{K(n, q) \cdot |\mathbf{C}_y|^n} \quad (6)$$

为计算方便，对上式两边取对数得：

$$L(\mathbf{C}_x | \mathbf{C}_y) = -n \ln |\mathbf{C}_x| - ntr(\mathbf{C}_y^{-1} \cdot \mathbf{C}_x) + (n-q) \ln |\mathbf{C}_x| - \ln K(n, q) \quad (7)$$

设 \mathbf{C}_y 为第 y 类的类别中心且 $y \neq x$ ，在没有先验知识的情况下，对式(7)两边取反并去掉非依赖项，定义协方差矩阵 \mathbf{C}_x 到 \mathbf{C}_y 的距离为

$$d(\mathbf{C}_x, \mathbf{C}_y) = \ln |\mathbf{C}_y| + tr(\mathbf{C}_y^{-1} \cdot \mathbf{C}_x) \quad (8)$$

依据最大似然判别准则，对于当前协方差矩阵 \mathbf{C}_x ，若 $d(\mathbf{C}_x, \mathbf{C}_y)$ 是所有的 $y \in \{1, 2, \dots, m\}$ 且 $y \neq x$ 中最小的距离，则将 \mathbf{C}_x 判别到类别 y 中，此时表明矩阵 \mathbf{C}_x 和 \mathbf{C}_y 的相似性很大。故采用距离 d 作为其散射特性相似性的度量参数， d 越小则其相似性越大。

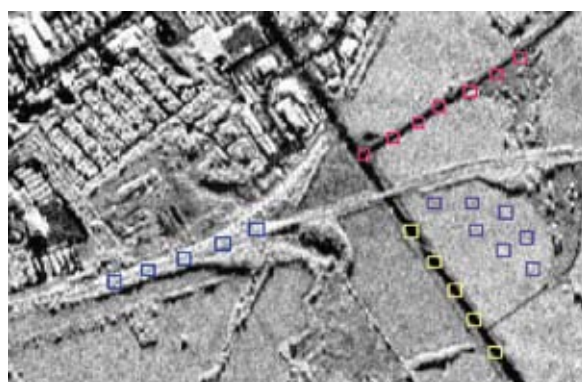


图1 SAR图像冗余信息

2.3 基于散射特性相似性的相干斑抑制

本文引入散射特性的相似性，根据相似性用全局极化数据的加权平均值恢复待处理极化数据的散射特性。权值的取值依赖于散射特性的相似性，相似性越大，则平均时所选取的权值越大，即散射特性相似性

大的数据在待处理数据的恢复过程中贡献大。相干斑抑制过程可由下式表示

$$NL(C_x) = \frac{1}{Z(x)} \sum_{C_y \in Y} w(C_x, C_y) C_y \quad (9)$$

式中, C_x 表示待处理的协方差矩阵; C_y 表示在当前滤波窗口中除 C_x 外其他所有的协方差矩阵; $w(C_x, C_y)$ 表示加权平均时所取的权重, 如式(10)所示, 它的大小依赖于 C_x 和 C_y 之间的相似性, 相似性越大 $w(C_x, C_y)$ 值越大。加权的权重表达为:

$$w(C_x, C_y) = \exp\left(-\frac{(\ln|C_y| + \text{tr}(C_y^{-1}C_x))^2}{h^2}\right) \quad (10)$$

式中, 归一化因子 $Z(x)$ 为

$$Z(x) = \sum_{C_y \in Y} \exp\left(-\frac{(\ln|C_y| + \text{tr}(C_y^{-1}C_x))^2}{h^2}\right) \quad (11)$$

式中, h 是一个控制滤波程度的经验参数。

2.4 算法实现过程与步骤

在计算滤波窗口中各矩阵与待处理矩阵间的距离时, 先以待处理矩阵为中心, 选取较小的窗口作为邻域窗口; 接着以滤波窗为界限滑动此邻域窗, 并记为搜索窗。滤波窗口的每一矩阵先后都会成为搜索窗的中心数据, 该中心数据与待处理矩阵间的距离用其所属的搜索窗与邻域窗中各相同位置所对应的极化数据间距离的均值来代替。本文滤波算法步骤如下:

步骤1 解压原始多极化SAR图像数据, 获得目标极化散射特性;

步骤2 因为滤波窗口选择较大增强滤波, 较小则可以保持细节信息。实验中选取滤波窗口的大小为 5×5 ; 邻域窗的大小为 3×3 , 即搜索窗的大小; 平滑参数 h 取0.5;

步骤3 在滤波窗口内滑动搜索窗, 利用式(8)计算每一搜索窗的中心矩阵与待处理协方差矩阵之间的距离, 此距离用搜索窗中每一矩阵与邻域窗各相同位置所对应的矩阵间的距离的均值代替;

步骤4 将步骤3得到的距离代入式(10)来获得滤波窗口内每一矩阵与待处理矩阵加权平均时的权值, 实现相似性度量;

步骤5 利用式(9)在滤波窗口内由权值对方差矩阵进行加权平均, 得到待处理矩阵元素的恢复值;

步骤6 按照上述步骤, 对方差矩阵各个元素进行相同处理, 再根据式(4)计算极化总功率, 并通过极化合成方式得到相干斑滤波前后的伪彩色合成图。

3 实验结果及分析

3.1 相干斑抑制效果评估与分析

为了客观地评价相干斑抑制效果, 本文采用以下几个指标对其进行评估:

(1) 等效视数(ENL)是衡量SAR图像相干斑的相对强度指标(王晓军等, 2004)。在一均匀区域其定义为:

$$\text{ENL} = \frac{\mu^2}{\sigma^2} \quad (12)$$

式中, μ 和 σ 分别是图像局部均值和标准差。ENL越大表明相干斑抑制的效果越好。定义相干斑抑制因子 β 为:

$$\beta = \frac{1}{\sqrt{\text{ENL}}} \quad (13)$$

β 越小说明抑制效果越好。

(2) 均值偏差(Devi)是细节保持程度的指标(汪洋等, 2009)。其定义为

$$\text{Devi} = \frac{\mu_i' - \mu_i}{\mu_i} \quad (14)$$

式中, μ_i 、 μ_i' 分别是滤波前后图像的均值。图像没有经过任何处理时 $\text{Devi} = 0$ 。经过滤波处理后其值越接近于零, 表明对图像的细节保持得越好。

(3) 目标的极化特征图可以比较相干斑抑制前后极化信息的保持情况。该特征图反映的是SAR天线在任意极化组合下的接收功率, 即

$$P(\delta_r, \varphi_r, \delta_t, \varphi_t) = k'(\lambda, \theta, \varphi) \mathbf{J}_r^T \mathbf{K}' \mathbf{J}_t \quad (15)$$

式中, (δ_r, φ_r) 、 (δ_t, φ_t) 是接收电磁波和发射电磁波的极化椭圆参数, δ_r 和 φ_r 分别表示发射天线的椭圆率角和方位角。 $k'(\lambda, \theta, \varphi)$ 是与天线有效面积和波导抗有关的常数, \mathbf{J}_r 和 \mathbf{J}_t 分别描述了天线在 (δ_r, φ_r) 、 (δ_t, φ_t) 状态的Stokes的极化矢量, 与目标散射无关, \mathbf{K}' 为目标的Kennaugh矩阵, 上标“T”表示向量的转置。若只关心接收功率的相对值, 可省略常数 $k'(\lambda, \theta, \varphi)$ 来简化计算。发射天线和接收天线的极化状态可以在有效范围内任意取值。当 $\delta_r = \delta_t$ 、 $\varphi_r = \varphi_t$ 时, 这种两者极化一致

的状态称为同极化；当 $\delta_r = -\delta_t$ ， $\varphi_r = \pi - \varphi_t$ 时，这种极化正交的状态称为交叉极化。由电磁波的接收功率可得到三维极化特征图，由上可知，该特征图是由目标的Kennaugh矩阵决定，而目标的极化信息又包含在Kennaugh矩阵之中，故可用极化特征图来表征目标的极化信息。

3.2 多极化SAR图像相干斑抑制实验

以下实验使用的测试数据是由美国喷气推进实验室(NASA/JPL) AIRSAR L波段获得的旧金山海湾的全极化数据。该成像区域分别由图像左上区域的太平洋、右上区域的金门桥以及右下方的旧金山市区组成。数据区域大小选取为 512×512 。分别对其进行PWF、极化Lee滤波和本文方法的滤波处理，图2列出了该测试数据处理后的极化伪彩色合成图像。

由目视效果来看，几种方法对SAR图像的相干斑都有一定程度的抑制作用。但PWF滤波效果并不理想，尤其是海平面匀质区域相干斑仍很明显，这是因为PWF须通过组合各极化通道数据来得到去斑图像。极化Lee滤波对相干斑有较好的抑制，但在市区细节较多的区域信息损失较严重，如图2(c)所示下方小圆圈内细节已经模糊。这是由于极化Lee滤波的抑制效果受滤波窗口大小的影响，窗口较小则相干斑抑制不明显，窗口较大则细节保持能力较差。此

外，以上两种方法都引入了通道间串扰(周晓光 等，2008)，导致极化信息的丢失。新提出的方法与PWF和极化Lee滤波方法相比有更好的滤波效果：首先图像左上区域结构较简单，相干斑更少，图像更平滑，如图2(d)中左方框所示；其次，图像下方区域结构复杂，细节更多，线结构更清晰，如图2(d)中小圆圈所示。为了更好地比较细节保持能力，图2(e)一(h)是图2(a)右方框经各种方法处理后对应的细节放大图。从图中可看出，图2(h)的细节更突出图像质量更好。

从整体和局部来看，本文方法都明显好于现有PWF和极化Lee滤波，该方法是对协方差矩阵各个元素单独处理，故能更好地保留极化信息。图3分别显示图2(a)中左方框所对应的原始和经本文方法处理后数据的极化特征图。由图可知，无论是同极化还是交叉极化，处理后的极化特征图与原始的极化特征图具有较强的一致性，证明了本文方法得到的图像在整体上极化信息保持较好。

利用上述等效视数和均值偏差两种指标对滤波效果进行定量评估。首先对相干斑抑制程度进行量化，利用PWF、极化Lee滤波与本文方法处理测试数据，将图2(a)中左方框所对应的各匀质区域的 σ 、 μ 、ENL和 β 具体数值记录如表1所示。其次评估图像细节的保持程度，几种方法处理后的伪彩色合成图与原始图的Devi值如表2所示。

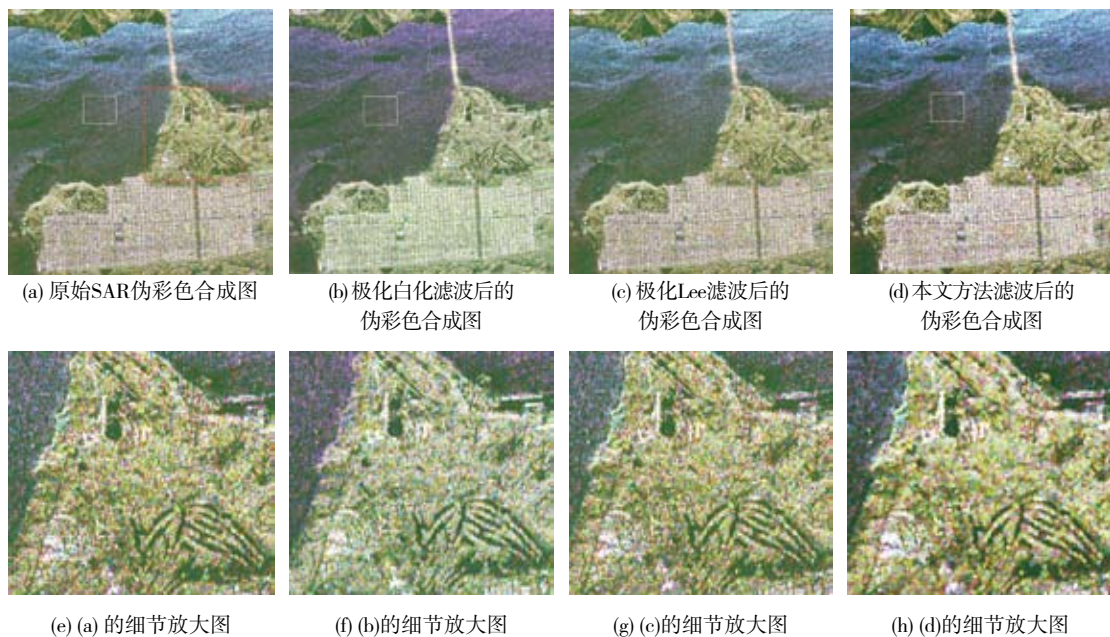


图2 SAR图像滤波结果

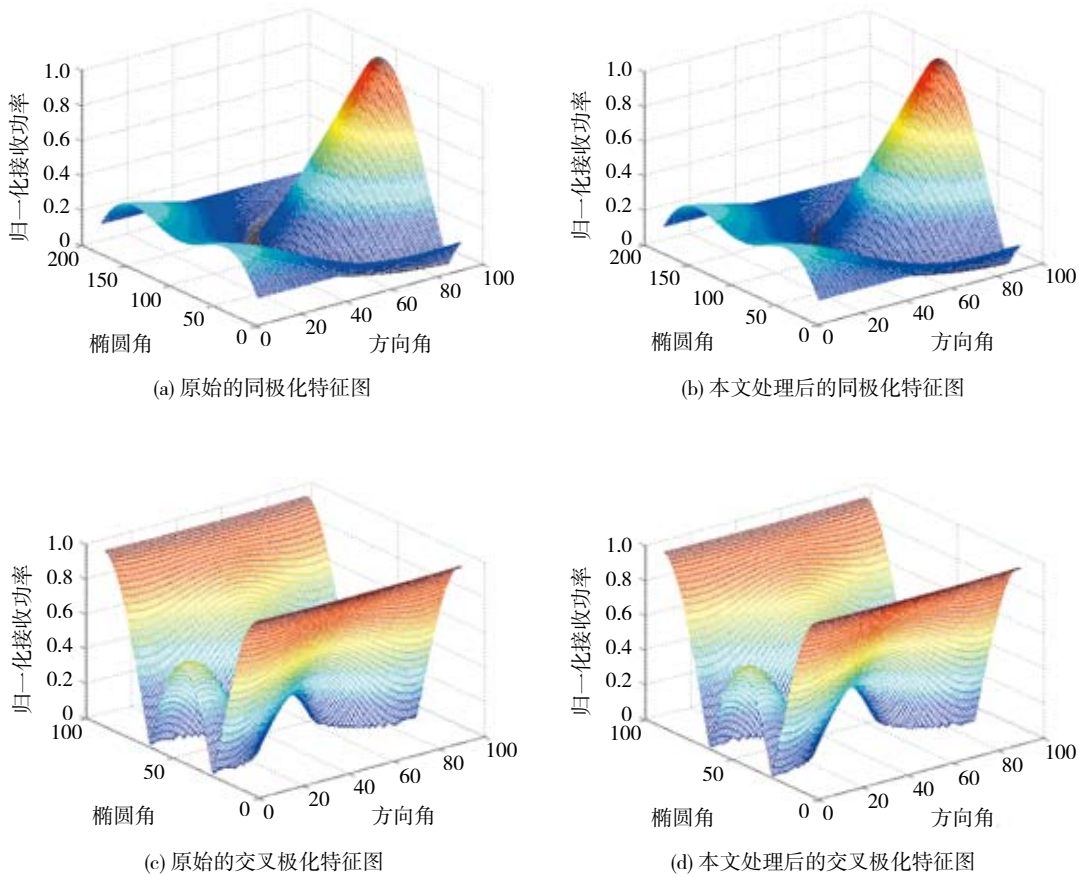


图3 极化特征图

表1 在相干斑抑制程度方面的比较

	原始图	PWF滤波	极化Lee滤波	本文方法
σ	55.7696	54.1479	54.9324	40.9214
μ	127.3470	92.6229	128.2230	120.3650
ENL	5.2142	2.9260	5.4485	8.6518
β	0.4379	0.5846	0.4284	0.3400

表2 在细节保持方面的比较

	原始图	PWF滤波	极化Lee滤波	本文方法
Devi	-0.0251	-0.0276	-0.0207	-0.0200

由表中数据可看出新提出方法处理后图像的 σ 最小, ENL最大, 且 β 值最小, 其相干斑抑制能力最强; Devi值最接近于0, 表明本文方法对图像的细节保持能力最好。

4 结论

提出一种新的多极化SAR图像的相干斑抑制方法。通过分析多极化SAR图像数据散射特性的相似性, 并引入极化域加权平均的滤波思想, 结合多极化SAR数据协方差矩阵的Wishart分布, 推导出了散射特性相似性的度量参数。对真实SAR图像数据的测试结果表明, 该方法与传统极化滤波方法相比, 在相干斑抑制能力及图像细节保持程度方面均有较大提高。其突出特点在于能对协方差矩阵的各个元素独立滤波, 故在极化信息的保留上具有潜在优势, 也更加便于多极化SAR图像后续处理。需要指出的是, 在SAR图像相干斑严重时, 将影响搜索窗口中散射特性相似性的度量, 今后将进一步研究如何减少相干斑对相似性度量的影响。

参考文献(References)

- Buades A, Coll B and Morel J M. 2005a. Image denoising by non-local averaging. 2005 IEEE International Conference on Acoustics Speech and Signal Processing. New York: IEEE, 2: 25–28 DOI: 10.1109/ICASSP.2005.1415332
- Buades A, Coll B and Morel J M. 2005b. A review of image denoising algorithms, with a new One. Multiscale Modeling and Simulation, 4(2): 490–530 DOI: 10.1137/040616024
- Bouchemakh L, Smara Y and Boutarfa S. 2008. A comparative study of speckle filtering in polarimetric radar SAR images. Proceedings of the International Conference on Information and Communication Technologies from Theory to Applications ICTTA' 08. New York: IEEE: Piscataway, NJ, USA: 1–6 DOI: 10.1109/ICTTA.2008.4530040
- 江勇, 张晓玲, 师君. 2009. 极化SAR改进Lee滤波相干斑抑制研究. 电子科技大学学报, 38(1): 5–8
- Lee J S, Grunes M R and De Grandi G. 1999. Polarimetric SAR speckle filtering and its implication for classification. IEEE Trans Geoscience and Remote Sensing, 37(5): 2363–2373 DOI: 10.1109/36.789635
- 刘秀清, 杨震, 杨汝良. 2003. 全极化合成孔径雷达图像极化白化滤波参数估计方法的改进研究. 电子学报, 31(12): 1795–1799
- 迈特尔, 孙洪. 2005. 合成孔径雷达图像处理. 北京: 电子工业出版社: 28–30
- 迈特尔, 孙洪, 管鲍. 2004. SAR图像相干斑抑制滤波性能评价. 系统工程与电子技术, 26(9): 1165–1171
- Oliver C and Quegan S. 1998. Understanding Synthetic Aperture Radar Images. Boston: Artechhouse: 209–212
- 皮亦鸣, 邹琪, 黄顺吉. 2002. 极化SAR相干斑抑制——极化白化滤波器. 电子与信息学报, 24(5): 597–603
- Touzi R and Lopes A. 1994. The principle of speckle filtering in polarimetric SAR imagery. IEEE Transactions on Geoscience and Remote Sensing, 32(5): 1110–1114 DOI: 10.1109/36.312901
- Wang X J, Sun H and Guan B. 2004. Evaluation for coherent speckle suppression filters of SAR images. Systems Engineering and Electronics, 26(9): 1165–1171
- 汪洋, 鲁加国, 张芬. 2009. 一种新的极化滤波综合性能评估方法. 无线电工程, 39(4): 37–40
- Yang X Z and Clausi D A. 2009. Structure-preserving speckle reduction of SAR images using nonlocal means filters. Image Processing (ICIP), 2009 16th IEEE International Conference on. New York: IEEE, 345 E 47Th St, New York, NY 10017 USA: 2985–2988
- 周晓光, 匡纲要, 万建伟. 2008. 多极化SAR图像斑点抑制综述. 中国图象图形学报, 13(3): 377–385
- 朱良, 郭巍, 禹卫东. 2009. 合成孔径雷达卫星发展历程及趋势分析. 现代雷达, 31(4): 5–10